Blow-up dynamics for the aggregation equation with degenerate diffusion

Yao Yao[a], Andrea L. Bertozzi[a]

[a]Department of Mathematics, University of California Los Angeles, Los Angeles, CA 90095, USA

Abstract

We study radially symmetric finite time blow-up dynamics for the aggregation equation with degenerate diffusion $u_t = \Delta u^m - \nabla \cdot (u * \nabla(K * u))$ in $\mathbb{R}^d$, where the kernel $K(x)$ is of power-law form $|x|^{-\gamma}$. Depending on m, d, γ and the initial data, the solution exhibits three kinds of blow-up behavior: self-similar with no mass concentrated at the core, imploding shock solution and near-self-similar blow-up with a fixed amount of mass concentrated at the core. Computation are performed for a variety of m, d and γ using an arbitrary Lagrangian Eulerian method with adaptive mesh refinement.

Key words: blow-up, self-similarity, aggregation, degenerate diffusion

1. Introduction

1.1. Background

Aggregation-diffusion type equations arise in a wide variety of biological applications, such as Patlak-Keller-Segel (PKS) models of chemotaxis and migration patterns in ecological systems. In this paper, we study finite-time blow-up in the following equation

$$u_t = \Delta u^m - \nabla \cdot (u\nabla(K * u)) \quad \text{in } [0,T) \times \Omega, \tag{1.1}$$

with Neumann boundary condition, where $m \geq 1$, $\Omega = B(0,R) \subset \mathbb{R}^d$, and K is a radially symmetric potential with power-law form, i.e.

$$K(x) = \frac{1}{|x|^\gamma},$$

where K is either equal to or less singular than the Newtonian kernel at the origin, i.e. $\gamma \leq d-2$.

Equation (1.1) is used as a model for various biological and physical phenomena (see [H] for a review). In particular, when K is the Newtonian potential, i.e. $\gamma = d-2$ for $d \geq 3$, (1.1)

Email addresses: `yaoyao@math.ucla.edu` (Yao Yao), `bertozzi@math.ucla.edu` (Andrea L. Bertozzi)

Preprint submitted to Elsevier *March 5, 2012*

becomes the Patlak-Keller-Segel equation with degenerate diffusion, which describes motion of a species by chemotaxis: here u represents the density of the bacteria, and $K * u$ represents the density of the chemo-attractant. It is well known that the solution of (1.1) exhibits different behavior for different powers of m [DP, HV, S1, BCM]: the problem is *supercritical* for $1 \leq m < 2 - 2/d$, where the solution may exhibit finite time blow-up phenomena; while for $m > 2 - 2/d$ the problem is *subcritical* and the solution is globally bounded for all time. Recently the notion of criticality is generalized to general power-law kernels $K = \frac{1}{|x|^\gamma}$ in [BRB]. For $d \geq 3$ and $\gamma \leq d - 2$, they prove that the critical power m is given by $\frac{d+\gamma}{d}$. When $m > \frac{d+\gamma}{d}$ the solution stays uniformly bounded for all time, while when $m < \frac{d+\gamma}{d}$ there may be a finite-time blow-up. Moreover, at the critical power, they prove that there exists a critical mass M_c which sharply divides the possibility of finite time blow up and global existence.

In this paper we only discuss the case $d \geq 3$, and the reason to omit dimension $d = 2$ is as follows. When $d = 2$, if K is equal to the Newtonian potential $\frac{1}{2\pi} \ln |x|$, the critical exponent is given by $m = 1$, and (1.1) becomes the original Patlak-Keller-Segel equation, which has been well studied both asymptotically and numerically [BCKSV, HV, CS, L]; if K is less singular than the Newtonian potential, then for any $m \geq 1$, the problem is in the subcritical regime, where all solutions have a global L^∞ bound and do not blow-up.

Once the existence/blow-up results are proven for (1.1), it is natural and interesting to examine the asymptotic behavior of the blow-up profile. Existing results only cover the following two special cases: one is the case without the diffusion term, and the other case is where K is the Newtonian potential. We review these cases in detail in the following discussion. The main goal of this paper is to study the behavior of the blow-up solution for general power-law kernel and power-law degenerate diffusion.

In the absence of the diffusion term Δu^m, (1.1) becomes the aggregation equation, which arises in biological swarming models and aggregation in material science. It is rigorously proved in [BCL1] that the local vs. global well-posedness is distinguished by an Osgood condition on the kernel K. In particular, when the kernel K is given by $|x|^\gamma$, the solution has a finite time blow-up for $0 < \gamma < 2$, and has an infinite time blow-up for $\gamma \geq 2$. For this power-law kernel, some asymptotic results for radial blow-up solutions are obtained in [HB1, HB2]: when $\gamma < 2$, they show the radial solution blows up in finite time and exhibits a second type self-similarity, while for $\gamma > 2$ the aggregation happens in infinite time and exhibits a concentration of mass along a collapsing δ-ring. We point out a difference of the self-similar blow-up between (1.1) and the aggregation equation: although (1.1) and the aggregation equation both exhibit self-similar blow-up behavior, the self-similarity for aggregation equation is of second type, while the self-similarity for (1.1) is indeed of first type. This is because in (1.1) the three terms u_t, Δu^m and $\nabla \cdot (u \nabla (K * u))$ should be of the same order, which gives one more equation than the aggregation equation and thus uniquely fixed the scaling.

With the presence of a linear diffusion term Δu, when K is the Newtonian potential, the problem is supercritical when $d > 2$, and critical when $d = 2$. For $2 < d < 10$, the asymptotic blow-up behaviors are carefully studied in [BCKSV]. They showed that there are two stable blow-up modality, one is self-similar and the other one is non-self-similar and Burger-like. When $d = 2$ the blow-up behavior is more subtle. For critical mass $M = M_c$, it is shown in [KS] that the L^∞ norm of solution grows to infinity as $t \to \infty$, where $u_{\max} \sim e^{2\sqrt{2t}}$. For supercritical mass $M > M_c$, according to asymptotic expansions computed in [CS, L] (and [HV] for a similar model), as $t \to T$, the solution is "near-self-similar" and blows up in the form

$$u(r,t) \sim R(t)^2 \bar{u}(rR(t)) + 1_{\{r>R(t)\}} f(r), \tag{1.2}$$

where $R(t) \sim (T-t)^{-1/2} g(T-t)$, where $g(T-t)$ is some logarithmic correction term; and $f(|x|)$ is some locally integrable function in $\mathbb{R}^2$ which has a singularity at the origin.

When the equation (1.1) has a nonlinear diffusion term Δu^m and Newtonian potential K, the problem is *critical* when $m = 2 - 2/d$, where $d \geq 3$. For solutions with supercritical mass $M > M_c$, some results regarding the asymptotic behavior of blow-up solution are obtained in [BL]: they prove that there exists a self-similar blow-up solution when the mass ranges in some bounded interval $(M_c, M_2]$ for some threshold M_2, however the stability of those self-similar blow-up solutions remains unclear. When the mass is above M_2, they prove that there is no exact self-similar blow-up solution, and the blow-up scaling is still open.

This paper uses refined numerics compared with asymptotic analysis to understand blowup behavior in a radially symmetric setting. Thus for completeness we review related numerical results, many of which do not discuss the blow up problem. There are a number of approaches to solving (1.1) for the special case $m = 1$ and K being a Newtonian potential. These methods include the finite-element or discontinuous Galerkin methods presented in [E, EI, EK, Fi, M, Sa, SS], the moving mesh method described in [BCR], a mass-transport steepest descent scheme in [BCC], a stochastic particle approximation method in [HS], and a composite particle-grid numerical method in [Fa]. However, among those approaches, few of them compute the blow-up profile: since (1.1) can blow-up in finite time in a diminishing length scale, it is a challenging numerical problem to capture the solution behavior precisely. There are two papers [BCKSV] and [BCR] directly addressing the blow-up profile, and both of their numerical methods rely on K being Newtonian: [BCKSV] directly solves for the mass function $M(r,t) := \int_0^r u(r) r^{d-1} dr$, which satisfies a local PDE when K is Newtonian; [BCR] deals with the parabolic-parabolic Keller-Segel problem, where the drift potential can be directly solved from a parabolic PDE. Their methods no longer work when K is a general power-law kernel $|x|^{-\gamma}$, and some efficient way to compute the convolution $K * u$ is needed.

1.2. Summary of Results

As we mention above, there are few results addressing the dynamic behavior of the blow-up solutions to (1.1), and that motivates our study. Sections 2-4 investigate the possible asymptotic behavior of blow-up solutions to (1.1), and formally show that there are three different ways of blow-up. These asymptotic results are accompanied by numerical simulations, and in Section 5 we outline our numerical method, which is an arbitrary Lagrangian Eulerian method with adaptive mesh refinement. Our results are summarized below.

Asymptotics for blow-up solutions with supercritical power m (i.e. $1 \leq m < \frac{d+\gamma}{d}$)

For supercritical m, we show that there are two kinds of possible blow-up behaviors. One of them is self-similar, where the scaling of the blow-up is

$$u(x,t) \sim (T-t)^{-\beta} w\left(\frac{x}{(T-t)^\alpha}\right) \text{ as } t \to T, \tag{1.3}$$

where the power $\alpha, \beta > 0$ are computed in Section 2 (see (2.2)). We point out that as t approaches the blow-up time T, the mass of the peak area goes to zero, indicating that no mass is concentrating at the origin.

Another possible blow-up behavior is an imploding smoothed out shock wave which collapses into a Dirac mass at the origin at the blow-up time. More specifically, u forms a delta concentration on an imploding spherical surface, thus the mass function $M(r,t) := \int_0^r u(y,t)y^{d-1}dy$ is forming an imploding shock. In Section 3 we show that the scaling associated to this kind of blow-up is

$$u(r,t) \sim Q(t)\ \varphi\left(\frac{r-R(t)}{\delta(t)}\right) \tag{1.4}$$

where $\lim_{t\to T} Q(t) = \infty$, $\lim_{t\to T} R(t) = 0$, and $\delta(t) \ll R(t)$ as $t \to T$. We compute the scaling for $Q(t), R(t)$ and $\delta(t)$ in Section 3.1 (see (3.6) and (3.9)), and derive the equation satisfied by φ in Section 3.3. We point out that while the same blow-up behavior is discovered in [BCKSV] for $m = 1$ and Newtonian K, this is the first work to find out the blow-up profile φ. Note that in this case a finite amount of mass is driven to the origin at the blow-up time, indicating that this type of blow-up is intrinsically different from the self-similar blow-up.

Another difference between the two type of blow-up is as follows. As long as $1 < m < \frac{\gamma+d}{\gamma}$ is in the supercritical regime, the self-similar blow-up can happen for any m, d, γ with a suitable initial data. However the non-self-similar blow-up requires an extra condition: in Section 3.2, we formally derive that the non-self-similar blow-up can only happen when the extra condition $\gamma > d-3$ is satisfied, in addition to m being supercritical. Numerical evidence suggests that this extra condition is indeed required. Note that when both conditions are satisfied, the blow-up behavior depends on the initial data: the solutions with radially decreasing initial data may tend to blow-up self-similarly, while solutions with ring-shaped initial data may tend to blow-up like a Burger shock.

Asymptotics for blow-up solutions with critical power m (i.e. $m = \frac{d+\gamma}{d}$)

When m is critical, numerical evidence suggests that u is self-similar in the peak region. However the maximum density here does not grow like $(T-t)^{-\beta}$ as in (1.3), and is $(T-t)^{-\beta}g(T-t)$ instead, where $g(T-t)$ is some logarithm correction. We assume that as $t \to T$, u is of the form

$$u(r,t) = \frac{1}{R(t)^d}\bar{u}(\frac{r}{R(t)}) + 1_{\{r>R(t)\}}f(r), \tag{1.5}$$

where $R(t) \ll (T-t)^\alpha$ as $t \to T$, here α is as in (2.2). We then obtain some preliminary results, indicating that $\bar{u}$ is the stationary solution to (1.1) with mass M_c. This implies that the mass in the peak area converges to M_c as $t \to T$, which is verified by numerical simulations. It is an interesting open problem to find the exact scaling for $R(t)$. We point out that this type of near-self-similar blow-up behavior is not new, and it is previously observed in the semilinear heat equation [GK] and Patlak-Keller-Segel problem in 2D [HV, CS, L].

Numerical method

In order to numerically compute the blow-up profile of (1.1), we use an arbitrary Lagrangian Eulerian method with adaptive mesh refinement. The main idea is to split equation (1.1) into two steps, one contains the aggregation part and the other contains the diffusion part. For the aggregation part, we adopt the method described in [HB1] and let the mesh move with the particles. The Lagrangian method is important for advection to avoid numerical diffusion [HB1]. Then we perform an adaptive mesh refinement and use an implicit finite volume scheme to solve the degenerate diffusion equation on a fixed mesh, due to its stability and easiness to implement. The advantage of our method is that we can compute the solution until the time is very close to the blow-up time, where the maximum density can be as large as 10^{80} and the characteristic spatial scale of the solution is 10^{-27}, while maintaining sufficient resolution to capture the detailed asymptotics of the blow-up profile.

2. Self-similar blow-up for supercritical power m

In this section we focus on the self-similar blow-up that happens for supercritical m, i.e. $m > \frac{d+\gamma}{d}$. Figure 1 gives a typical example of a self-similar blow-up, where no mass is concentrating at the origin as the time approaches the blow-up time. We determine the scaling for the blow-up, and formally derive the equation satisfied by the blow-up profile.

2.1. Computing the exponents

We assume that as $t \to T$, u blows up at the origin self-similarly with the following form

$$u(x,t) \sim (T-t)^{-\beta} w(\frac{x}{(T-t)^{\alpha}}) \text{ as } t \to T. \tag{2.1}$$

In this subsection, our goal is to compute the exponents α and β.

We first compute the order for the two term u_t and Δu^m as $t \to T$:

$$u_t \sim (T-t)^{-(\beta+1)},$$
$$\Delta u^m \sim (T-t)^{-2\alpha-\beta m}.$$

For the term $\nabla \cdot (u \nabla (u * K))$, we begin with estimating the order for $u * K$:

$$\begin{aligned} (u*K)(x,t) &= \int_{\mathbb{R}^d} (T-t)^{-\beta} w(\frac{y}{(T-t)^{\alpha}}) \frac{1}{|x-y|^{\gamma}} dy \\ &= (T-t)^{-\beta+\alpha d} \int_{\mathbb{R}^d} w(z) \frac{1}{|x - z(T-t)^{\alpha}|^{\gamma}} dz \quad (\text{let } z = \frac{y}{(T-t)^{\alpha}}) \\ &= (T-t)^{-\beta+\alpha d-\gamma\alpha} (w * \frac{1}{|x|^{\gamma}})(x(T-t)^{-\alpha}), \end{aligned}$$

which implies that

$$\nabla \cdot (u \nabla (u*K)) \sim (T-t)^{-2\alpha-2\beta+\alpha d-\gamma\alpha}.$$

Since we are looking for a self-similar blow-up profile, we want u_t, Δu^m and $\nabla \cdot (u \nabla (u*K))$ to have the same order, which gives the following equations

$$-(\beta+1) = -2\alpha - \beta m = -2\alpha - 2\beta + \alpha d - \gamma\alpha.$$

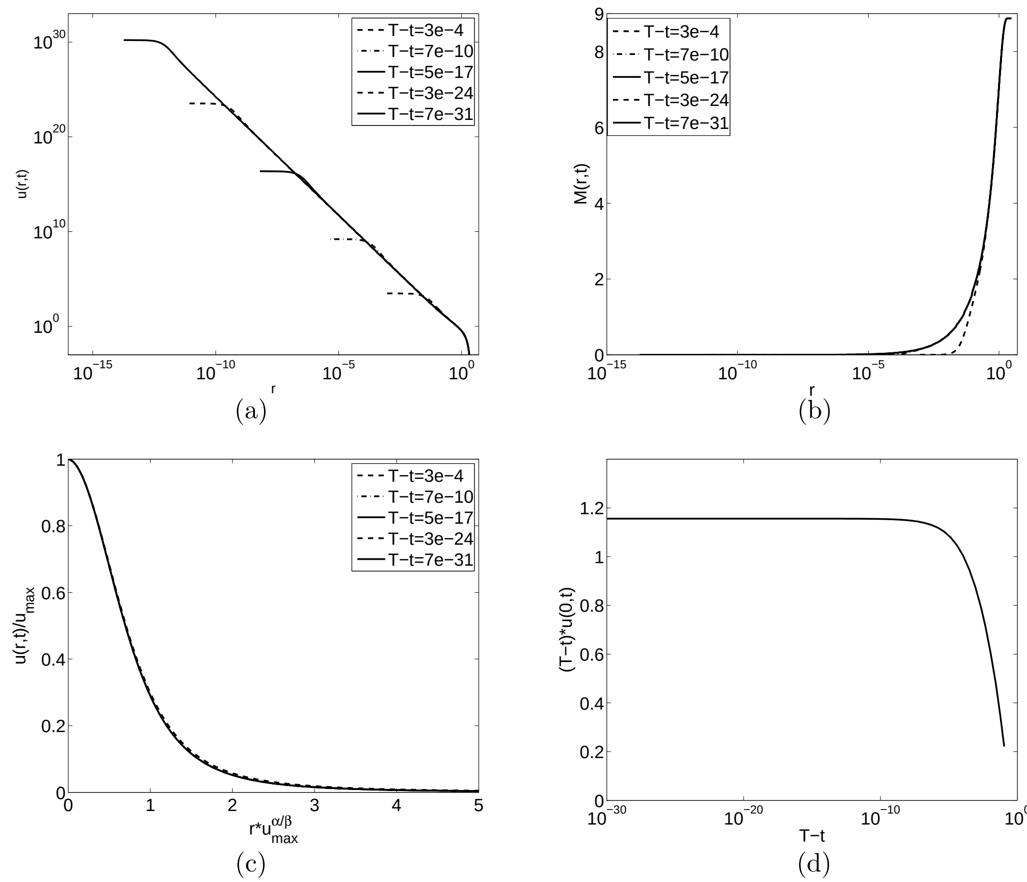

Figure 1: Time evolution of a self-similar blow-up solution with radially symmetric initial data, with Newtonian potential, $d = 3$ and $m = 1.2$ (supercritical). Figure (a) shows a log-log plot of the solution, which blows up at the origin at a finite-time T. Figure (b) shows the mass function $M(r, t)$ at different time, suggesting that no mass is concentrating at the origin as $t \to T$. Here $M(r, t)$ denotes the mass inside the ball $B(0, r)$ at time t. Figure (c) shows the rescaled solution, (here the scaling is determined in (2.2)), which converges to some blow-up profile. Figure (d) shows the evolution of $(T - t)u(0, t)$ as a function of $T - t$, which suggests that $u(0, t) \sim (T - t)^{-1}$ as $t \to T$.

Since there are two equations and two unknowns, we can explicitly solve for α, β in terms of γ, m and d:

$$\begin{cases} \alpha = \dfrac{2-m}{(m-1)(d-\gamma)-2(m-2)}, \\ \beta = \dfrac{d-\gamma}{(m-1)(d-\gamma)-2(m-2)}. \end{cases} \tag{2.2}$$

If the solution blows up, then α and β are both positive, which implies that the blow-up can only happen when $m < 2$. Also note that the mass in the ball $B(0, (T-t)^\alpha)$ is of the order $(T-t)^{-\beta+d\alpha}$, which cannot go to infinity as $t \to T$ since we start with a finite mass. This gives a necessary condition for the solution to blow-up, which is $-\beta + d\alpha \geq 0$, or in other words,

$$m \leq \frac{d+\gamma}{d}. \tag{2.3}$$

Note that $\frac{d+\gamma}{d}$ is exactly the critical exponent for (1.1) given by [BRB].

2.2. Self-similar blow-up profile

Assuming (2.1), we want to find the equation w satisfies. Plug w into (1.1), and let $y = x(T-t)^{-\alpha}$, we have that as $t \to T$,

$$\begin{aligned} u_t &\approx (T-t)^{-\beta-1}[\beta w(y) + \alpha y \cdot \nabla w(y)], \\ \Delta u^m &\approx (T-t)^{-2\alpha-\beta m} \Delta w(y), \\ \nabla \cdot (u \nabla (u * \frac{1}{|x|^\gamma})) &\approx (T-t)^{-2\alpha-2\beta+\alpha d-\gamma\alpha} \nabla \cdot (w \nabla (w * \frac{1}{|x|^\gamma}))(y). \end{aligned} \tag{2.4}$$

Therefore formally speaking, w should satisfies the following equation:

$$\beta w + \alpha y \cdot \nabla w = \Delta w^m - \nabla \cdot (w \nabla (w * \frac{1}{|x|^\gamma})). \tag{2.5}$$

Figure 2 shows the blow-up profile and scaling for different powers m, and Figure 3 illustrates that the blow-up profile indeed satisfies (2.5) for both Newtonian and non-Newtonian kernel K. It would be interesting to study the full behavior of (2.5), although it is outside the scope of this paper. The case for $m = 1$ and Newtonian potential V is covered in [BCKSV].

2.3. Limit function outside the blow-up region

From the numerical simulation in Figure 1(a), we can see that for every $r > 0$, $u(r,t)$ converges to some limit $\psi(r)$ as $t \to T$. Now we will formally compute the outer solution $\psi(r)$.

Since $\psi(r)$ is stationary as $t \to T$, we have that ψ satisfies the following equation, where we slightly abuse the notation and write ψ as a radially symmetric function on $\mathbb{R}^d$:

$$\nabla(\psi^{m-1} + \psi * \frac{1}{|x|^\gamma}) = 0. \tag{2.6}$$

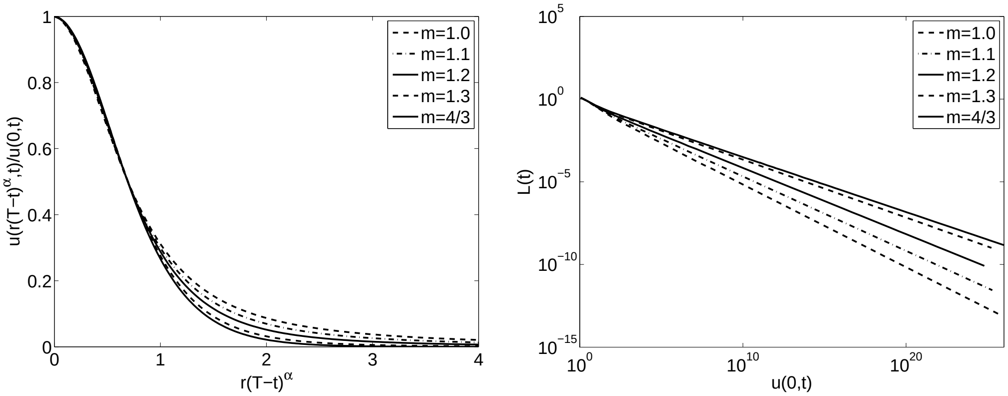

(a) (b)

Figure 2: Behavior of solutions with different power m, with Newtonian potential in $d = 3$. (a) Blow-up profile for different m. (b) log-log plot of the height $u(0,t)$ and the width $L(t)$ for different m, where $L(t)$ is defined as the radius at half the height of $u(0,t)$. The slopes of the lines are in good agreement with the theoretically predicted values of -0.5, -0.45, -0.4, -0.35 and $-1/3$.

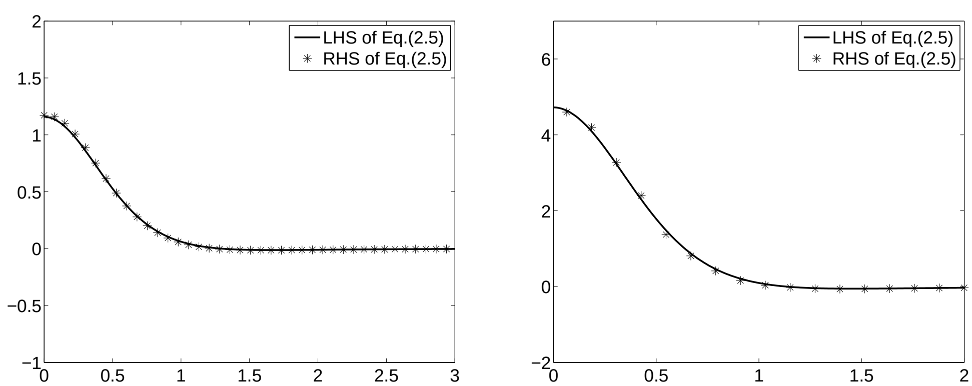

(a) (b)

Figure 3: Verification of Eq.(2.5) for the blow-up profile. The solid line is the plot of the left hand side of Eq.(2.5), and the stars represent the right hand side of Eq.(2.5). (a) Here the parameters are $m = 1.2$, $d = 3$ and $\gamma = 1$ (Newtonian). (b) Here the parameters are $m = 1.1$, $d = 3$ and $\gamma = 0.5$, where the kernel is less singular than the Newtonian kernel.

Since $\psi(r)$ appears to be a straight line on the log-log graph in Figure 1(a), we assume it takes the form $\psi(r) \sim r^{-a}$, where $a > 0$. Plug it into (2.6) and solve for a, we obtain $a = \frac{d-\gamma}{2-m}$, which implies the tail should satisfy

$$\psi(r) \sim r^{-\frac{d-\gamma}{2-m}}.$$

3. Non-self-similar blow-up for Supercritical Power m

When the initial data is not radially decreasing, it is possible for the solution to blow-up in finite time in a non-self-similar way. More precisely, the solution consists of an imploding smoothed out shock wave in the mass variable, which collapses into a delta function at the origin in finite time. Figure 4 gives an typical example of a non-self-similar blow-up.

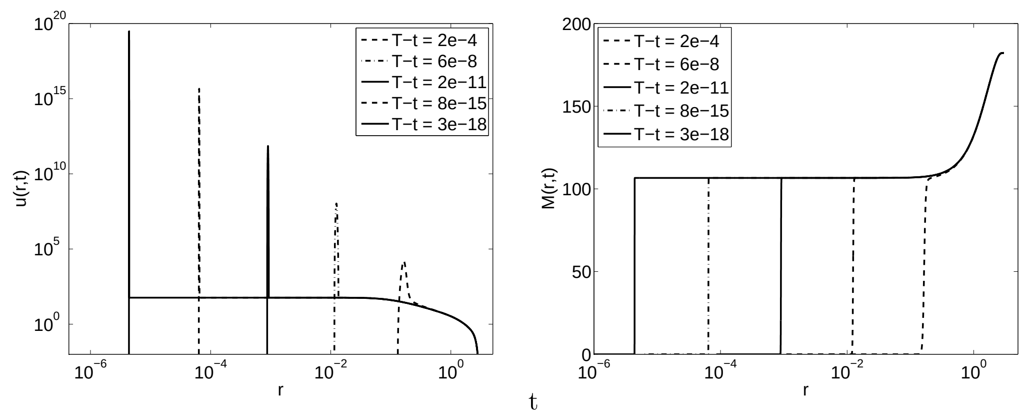

(a) (b)

Figure 4: Time evolution of a non-self-similar blow-up solution with radially symmetric initial data, with Newtonian potential, $d = 3$ and $m = 1.2$(supercritical). Figure (a) shows a log-log plot of the solution, which blows up at the origin at a finite-time T. Figure (b) shows the mass function $M(r,t)$ at different time, indicating that there is a fixed amount of mass concentrating at the origin as $t \to T$. Here $M(r,t)$ denotes the mass inside the ball $B(0,r)$ at time t.

We assume $u(r,t)$ have the following blow-up profile

$$u(r,t) \sim Q(t)\ \varphi\left(\frac{r - R(t)}{\delta(t)}\right), \tag{3.1}$$

where $\lim_{t\to T} Q(t) = \infty$, $\lim_{t\to T} R(t) = 0$, and $\delta(t) \ll R(t)$ as $t \to T$. Figure 5 shows the re-centered and rescaled solution indeed converge to some function φ.

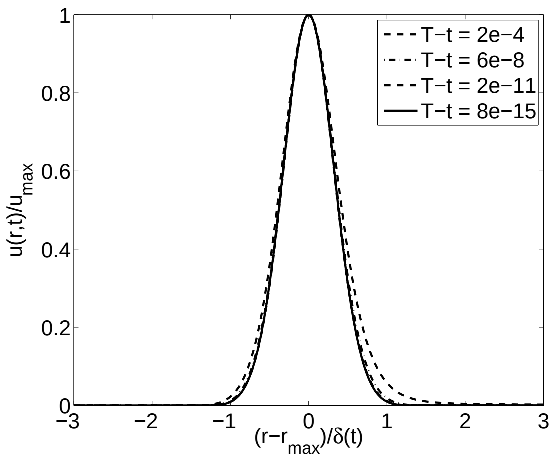

Figure 5: Simulation of a non-self-similar blow-up with radially symmetric initial data in three dimensions, with Newtonian potential and $m = 1.2$. The figure shows the re-centered and rescaled solution indeed converge to some function φ. The x-axis represents $(r - r_{max})/\delta(t)$, and the y-axis is the normalized density. Here $\delta(t)$ is computed according to (3.6).

3.1. Scaling for non-self-similar blow-up

We first figure out the relation between Q, δ and R. Since we only consider a radially symmetric solution, (1.1) can be written as

$$u_t = \underbrace{\partial_r^2 u^m}_{T_1} + \underbrace{\frac{d-1}{r}\partial_r u^m}_{T_2} - \underbrace{\partial_r u\ \partial_r(\frac{1}{|x|^\gamma} * u)}_{T_3} - \underbrace{u(\Delta\frac{1}{|x|^\gamma} * u)}_{T_4}. \tag{3.2}$$

Note that in the neighborhood of the peak, we have $\frac{1}{r}\partial_r u^m \sim Q^m/(R\delta)$ and $\partial_r^2 u^m \sim Q^m/\delta^2$, which gives $T_2 \ll T_1$, due to our assumption that $\delta(t) \ll R(t)$ as t goes to the blow-up time T. Thus T_2 becomes asymptotically irrelevant and can be ignored. We will require T_1, T_3, T_4 to be of the same size in the neighborhood of the peak. For T_1, the previous discussion gives

$$T_1 \sim \frac{Q^m}{\delta^2}. \tag{3.3}$$

We next estimate the order of T_4. When $\gamma < d - 2$, (i.e. the kernel is less singular than the Newtonian kernel), a direct computation gives

$$\Delta\frac{1}{|x|^\gamma} = \gamma(\gamma + 2 - d)\frac{1}{|x|^{\gamma+2}},$$

hence to obtain the order of T_4, it suffices to look at $(\frac{1}{|x|^{\gamma+2}} * u)(x)$ when $|x| - R(t) = O(\delta(t))$. For C large, we have

$$(\frac{1}{|x|^{\gamma+2}} * u)(x) \sim \int_{B(0,C\delta)} \frac{1}{|y|^{\gamma+2}} Q dy \sim Q\delta^{d-2-\gamma}. \tag{3.4}$$

hence when $|x| - R(t) = O(\delta(t))$, the computation above implies

$$T_4 \sim u\, (\frac{1}{|x|^{\gamma+2}} * u) \sim Q^2 \delta^{d-2-\gamma}. \tag{3.5}$$

Note that (3.5) holds for Newtonian kernel as well, since when $\gamma = d-2$, $\Delta|x|^{-\gamma}$ becomes a multiple of the delta function.

Finally, due to divergence theorem, we can evaluate the order of T_3 as follows

$$T_3 \sim \frac{Q}{\delta} \frac{1}{R^{d-1}} \int_{B(0,|x|)} \Delta \frac{1}{|x|^\gamma} * u dx.$$

Note that the integrand quickly vanishes to 0 as $|x| - R \gg \delta$. And when $|x| - R = O(\delta)$, the computation for T_4 yields that $\Delta|x|^{-\gamma} * u \sim \delta^{d-2-\gamma} u$, hence $\int_{B(0,|x|)} \Delta|x|^{-\gamma} * u dx \sim \delta^{d-2-\gamma} M$, where M is the mass of u around the peak. Recall that we assume that M is of order unity, which implies

$$T_3 \sim Q R^{1-d} \delta^{d-3-\gamma}.$$

Since we assume T_1, T_3, T_4 are of the same order, we finally obtain that $Q(t), R(t)$ and $\delta(t)$ should satisfy the following relation

$$R(t) \sim Q(t)^{-\frac{d-\gamma+m-2}{(d-\gamma)(d-1)}}, \quad \delta(t) \sim Q(t)^{\frac{m-2}{d-\gamma}}. \tag{3.6}$$

Now we compute the order of $Q(t)$ in terms of $T - t$, where T is the blow-up time. From the previous computation, when $|x| - R = O(\delta)$,

$$\text{RHS of (2.2)} \sim Q^{m - \frac{2(m-2)}{d-\gamma}}, \tag{3.7}$$

and the order of the left hand side is

$$\text{LHS of (2.2)} \sim \dot{Q} + Q \frac{d}{dt}(\frac{r - R(t)}{\delta(t)}) \sim \dot{Q} Q^{\frac{d+\gamma-md}{(d-\gamma)(d-1)}}. \tag{3.8}$$

Combining (3.7) and (3.8), we obtain

$$\dot{Q} Q^{\frac{d+\gamma-md}{(d-\gamma)(d-1)}} \sim Q^{m - \frac{2(m-2)}{d-\gamma}},$$

which implies

$$Q(t) \sim (T-t)^{-\frac{(d-\gamma)(d-1)}{(d-\gamma)(md-m-d+2)-(d-2)(m-2)}}. \tag{3.9}$$

In the special case of the Newtonian potential, $d - \gamma = 2$, and $Q(t)$ simplifies to $Q(t) \sim (T-t)^{-\frac{2(d-1)}{md}}$, which is in agreement with the result in [BCKSV] for the special case $m = 1$, and our work generalize their result to general m, d amd γ.

Figure 6(a) shows that when the solution blows up self-similarly, the maximum density $Q(t)$ indeed has the same scaling as (3.9). However, Figure 6(b) suggests that there is a difference between the Newtonian kernel and kernels less singular than Newtonian: for the Newtonian kernel (i.e. $\gamma = d-2$), numerical simulation suggests that $Q(t)(T-t)^{2(d-1)/md}$ converges to a constant as t goes to the blow-up time T, while for less singular kernel (i.e. $\gamma < d-2$) we have $Q(t)(T-t)^{-p}$ goes to 0 slowly as $t \to T$, where p is the power in (3.9).

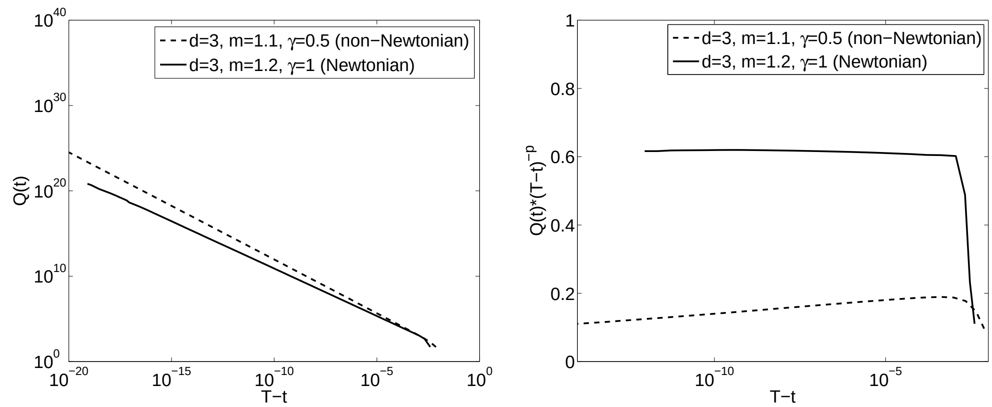

Figure 6: (a) Log-log plot of the maximum density $Q(t)$ versus $(T-t)$, where T is the blow-up time. The slopes of the lines are in good agreement with the theoretically predicted values in (3.9). (b) Plot of $Q(t)(T-t)^{-p}$ versus $(T-t)$, where p is the exponent as given in (3.9).

3.2. Requirements for the parameters

In this subsection, we derive some requirements for the parameters d, m and γ in order for the non-self-similar blow-up to happen. Recall that in (3.1), we assumed that $Q \to \infty, \delta \ll R \to 0$ as $t \to T$. Here $\delta \ll R \to 0$ as $t \to T$ implies that the following conditions on m, d and γ are required

$$m \leq \frac{d+\gamma}{d} \quad \text{and} \quad \gamma < d-2+m. \tag{3.10}$$

Note that the first requirement coincides with the criteria for supercritical m, hence is automatically satisfied in the supercritical regime. We point out that the second requirement can indeed be removed since we assume K is no more singular than the Newtonian potential at the origin, i.e. $\gamma \leq d-2$. Once the above conditions are met, $Q \to \infty$ as $t \to T$ will be automatically satisfied since $m \geq 1$.

Next we argue that an extra requirement is needed besides (3.10). Recall that in equation (3.4), we assumed that for $|x| = R + O(\delta)$, $(|x|^{-(\gamma+2)} * u)(x)$ is approximately equal to $\int_{B(0,C\delta)} |y|^{-(\gamma+2)} u(x-y)dy$ when C is of order unity and sufficiently large, which is comparable to $\delta^{-(\gamma+2)} Q \delta^d$. This requires that the tail of the kernel K be small such that the contribution from the term $\int_{\mathbb{R}^d \setminus B(0,C\delta)} |y|^{-(\gamma+2)} u(x-y)dy$ can be negligible, which implies that

$$\delta^{-(\gamma+2)} Q \delta^d \gg R^{-(\gamma+2)} Q R^{d-1} \delta,$$

which simplifies to the following extra requirement

$$\gamma > d-3. \tag{3.11}$$

Figure 7 provides numerical evidence that this extra requirement (3.11) is indeed valid. When all the conditions in (3.10) are met but not (3.11), even we start with a very singular ring-shaped initial data, the solution still behaves according to the scale for self-similar solution in Section 2, and eventually converges to a self-similar profile that is radially decreasing.

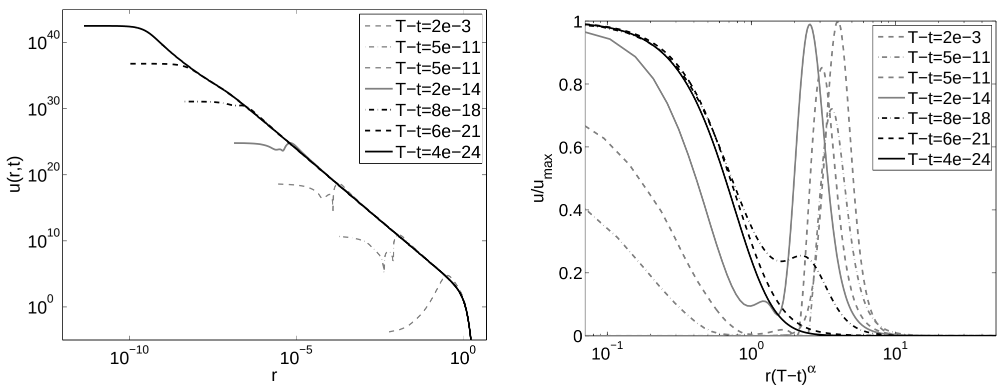

(a) (b)

Figure 7: Behavior of solutions with $d = 5, \gamma = 1$ and $m = 1.1$, where the condition (3.10) is satisfied but (3.11) is not. Even with a very singular ring-shaped initial data, it does not blow-up as an imploding shock. Figure (a) shows a log-log plot of the solution, which blows up at the origin at a finite-time T in a self-similar way with the scaling as in section 2. Figure (b) shows the rescaled solution, which eventually converges to some radially decreasing blow-up profile.

When both conditions (3.10) and (3.11) are met, the solution may blow-up in either a self-similar way or non-self-similar way, depending on its initial data. The examples shown in Figure 1 and 4 indeed have the same m, d and γ, and the only difference is that we start with a radially decreasing initial data in Figure 1 and a ring-shaped initial data in Figure 4. In Figure 8, we carefully choose the initial data that is close to the separatrix between the self-similar one and non-self-similar one. The blow-up turns out to be self-similar with the scaling as in Section 2, where the blow-up profile is not radially decreasing. We point out that this blow-up profile is unstable, and eventually the solution will be either attracted to a radially decreasing blow-up profile, or an imploding shock wave. This result is in agreement with [BCKSV] where $m = 1$ and K is Newtonian, where they conjectured that this separatrix has connection with the unstable blow-up modality that has exactly one linearly unstable mode.

3.3. Similarity Profile for Newtonian Kernel

When K is the Newtonian potential, when the solution blows up non-self-similarly according to (3.1), numerical evidence in Figure 5 suggests that the rescaled and re-centered solution converges to some blow-up profile φ. In this subsection, our goal is to find the equation that φ satisfies. We point out that this result is new even for Newtonian kernel: although the scaling of Q, R and δ has been studied in [BCKSV] for $m = 1$ and the Newtonian potential K, this is the first work to investigate the blow-up profile φ and find the equation it satisfies.

Let e_1 be the unit vector $(1, 0, \ldots, 0)$, and we investigate the behavior of solution to (1.1) near the point $((R(t) + y\delta(t))e_1, t)$, which corresponds to $\varphi(y)$. As $t \to T$, we have

$$u_t((R + y\delta)e_1, t) \approx \dot{Q}Q^{-\frac{2+md-2d}{2(d-1)}} \varphi'(y), \tag{3.12}$$

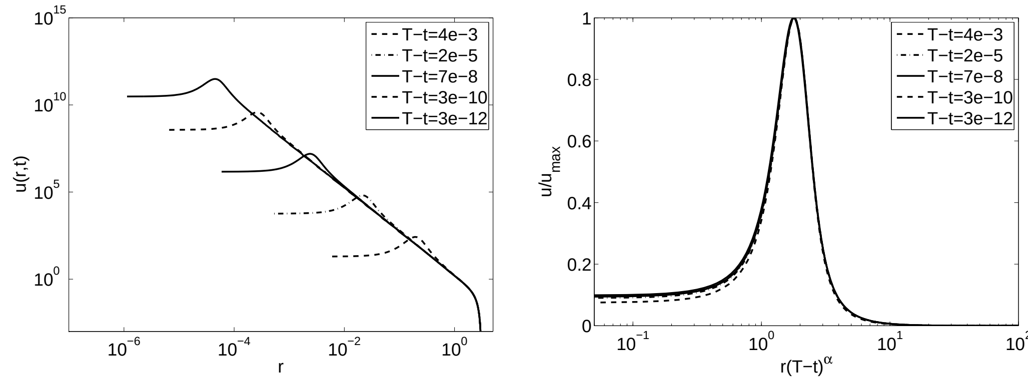

Figure 8: Blow-up profile in $d = 3$, $\gamma = 1$ and $m = 1.2$ (supercritical), with the initial condition chosen to be very close to the separatrix between the self-similar blow-up and non-self-similar blow-up. This blow-up profile is unstable and will be eventually attracted to either the non-self-similar blow-up or the self-similar blow-up with a radially decreasing profile. Figure (a) shows a log-log plot of the solution, and Figure (b) is the rescaled solution.

and

$$\Delta u^m((R + y\delta)e_1, t) \approx \frac{Q^m}{\delta^2}(\varphi^m(y))''. \tag{3.13}$$

The estimation of the last term $\nabla \cdot (u\nabla(u * K))$ is as follows. Note that when K is the Newtonian potential $\frac{1}{|x|^{d-2}}$, ΔK is $(2-d)\omega_{d-1}\delta(x)$ in the distribution sense, where $\delta(x)$ is the delta function and ω_{d-1} is the surface area of the sphere $\mathbb{S}^{d-1}$ in $\mathbb{R}^d$. Hence

$$\begin{aligned}
\frac{\partial}{\partial r}(u * \frac{1}{|x|^\gamma})(R + y\delta, t) &= \frac{\displaystyle\int_{B(0,R+y\delta)} \Delta u * \frac{1}{|x|^\gamma} dx}{|\partial B(0, R+y\delta)|} \\
&= \frac{(2-d)\displaystyle\int_{B(0,R+y\delta)} u dx}{R^{d-1}} \\
&\approx (2-d)\omega_{d-1} Q\delta \int_{-\infty}^{y} \varphi(z) dz,
\end{aligned}$$

where in the last line we used the fact that $u(r,t)$ is very small when $|r - R| \gg \delta$. and as a result,

$$\nabla \cdot (u\nabla(u * K))((R + y\delta)e_1, t) \approx (2-d)\omega_{d-1}\big(Q^2\varphi'(y)\int_{-\infty}^{y}\varphi(z)dz + Q^2\varphi^2(y)\big). \tag{3.14}$$

Combining (3.12), (3.13) and (3.14) together, we obtain that φ satisfies the following equation

$$-\frac{1}{d}\varphi'(y) = (\varphi^m(y))'' - (2-d)w_{d-1}\big(\varphi'(y)\int_{-\infty}^{y}\varphi(z)dz + \varphi^2(y)\big). \tag{3.15}$$

Figure 9 provides numerical evidence that the rescaled and re-centered blow-up profile indeed satisfies (3.15).

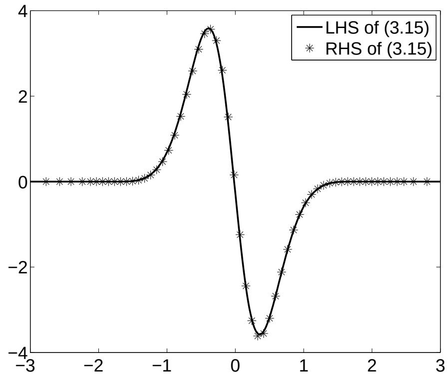

Figure 9: Verification of Eq.(3.15) for the blow-up profile of a non-self-similar blow-up, where $m = 1.2$, $d = 3$ and $\gamma = 1$. The solid line is the left hand side of Eq.(3.15), and the stars represent the right hand side of Eq.(3.15).

4. Near-self-similar blow-up for Critical Power m

When $m = \frac{d+\gamma}{d}$, it is proved in [BRB] that there exists a critical mass M_c depending on γ and d, such that the solution to (1.1) exists globally in time for $M < M_c$, while for any $M > M_c$ there exists a solution with mass M that blows up in finite time. In addition, for Newtonian potential, by using a comparison principle on the mass concentration, it is proved in [BK] that every radial solution with mass $M > M_c$ must blow up in finite time. We point out that their method can be generalized to the general power-law kernel $K = |x|^{-\gamma}$ as well.

In this section we let $m = \frac{d+\gamma}{d}$ be the critical power, and we study the blow-up behavior for solution with supercritical mass $M > M_c$. Let u be the weak solution to (1.1) with supercritical mass, which blows up at some finite time T. Figure 10 is a typical result of the simulation. While Figure 10(c) suggests that the blow-up is self-similar in its peak region, it is no longer of the form (2.1): suppose that u blows up with the form (2.1) as $t \to T$, then the same argument as in Section 2 would imply that the α and β given in (2.2) are the only possible exponents, and hence $(T-t)^\beta u(0,t)$ should converge to some finite number $w(0)$ as $t \to T$. However, numerical simulation of $(T-t)^\beta u(0,t)$ in Figure 10(d) suggests that this is not true, since $(T-t)^\beta u(0,t)$ is slowly increasing to infinity as $t \to T$, instead of converging to a constant.

Because of the self-similarity of u in the peak region, we assume that as $t \to T$, u is of the form

$$u(r,t) = \frac{1}{R(t)^d} \bar{u}(\frac{r}{R(t)}) + 1_{\{r>R(t)\}} f(r), \tag{4.1}$$

where $R(t) \ll (T-t)^\alpha$ as $t \to T$, here $\alpha = \frac{2-m}{(m-1)(d-\gamma)-2(m-2)}$ is as in (2.2).

It remains to determine $R(t)$, $\bar{u}$ and $f(r)$. If T is the blow-up time, we first introduce the following similarity variables

$$y = x(T-t)^{-\alpha}, \tau = -\ln(T-t),$$

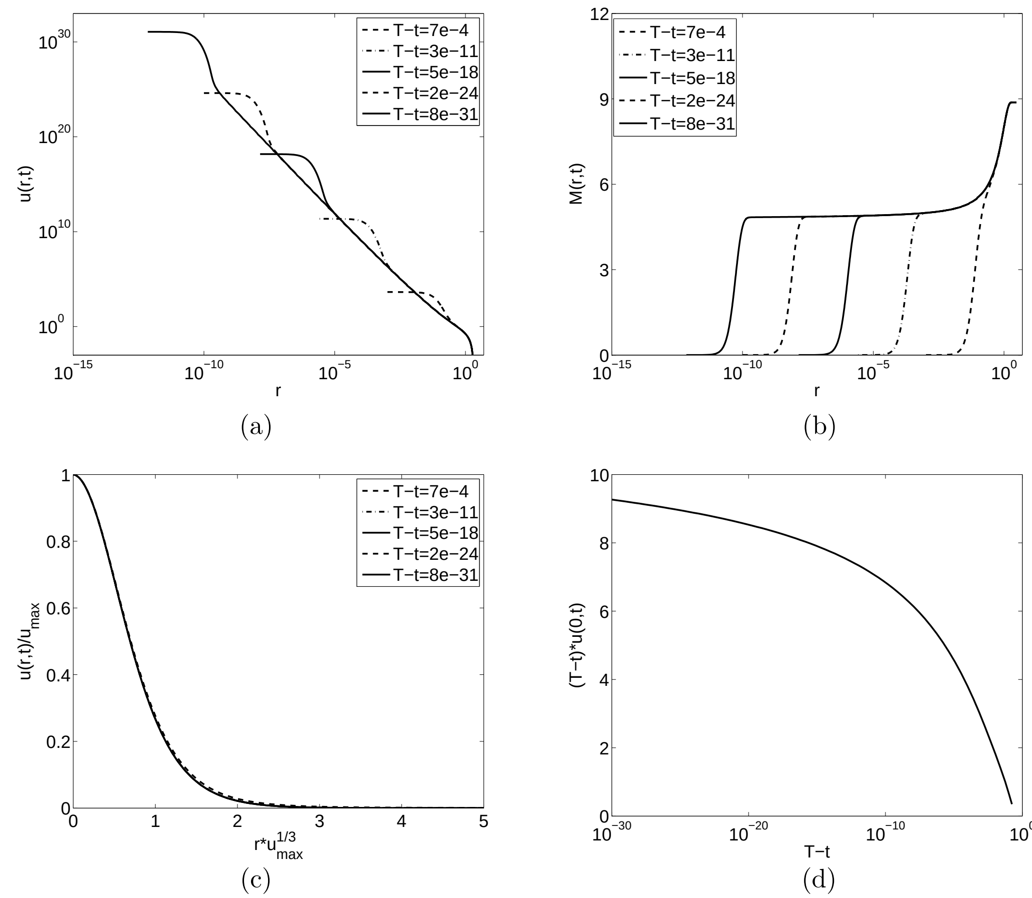

Figure 10: Time evolution of a near-self-similar blow-up solution with radially symmetric initial data, with Newtonian potential, $d = 3$ and $m = 4/3$ (critical). Figure (a) shows a log-log plot of the solution, which blows up at the origin at a finite-time T. Figure (b) shows the mass function $M(r,t)$ at different time, indicating that there is a fixed amount of mass contained in the peak area as $t \to T$. Here $M(r,t)$ denotes the mass inside the ball $B(0,r)$ at time t. Figure (c) is a rescaling of the peak area, which indicates that the peak area is self-similar and it converges to some profile. Figure (d) shows the evolution of $(T-t)u(0,t)$ as a function of $T-t$, which suggests that $u(0,t) \sim (T-t)^{-1} f(T-t)$ as $t \to T$, where f is some logarithmic correction term.

and $U(y,\tau) := (T-t)^{\beta} u(x,t)$, where α, β are given by (2.2). Then a quick computation reveals that $U(y,\tau)$ satisfies the following equation

$$U_\tau = \Delta U^m - \nabla \cdot (U \nabla (U * \frac{1}{|y|^\gamma})) - \alpha \nabla U \cdot y - \beta U. \tag{4.2}$$

Since we assume that $R(t) \ll (T-t)^\alpha$ as $t \to T$, we would expect that there is an inner layer of size $\epsilon(\gamma)$ in (4.2), where $\epsilon(\tau) \to 0$ as $\tau \to \infty$, however $\epsilon(\tau)$ should be bigger than any decaying power-law function as $\tau \to \infty$. Moreover, we expect that U is self-similar in this inner-layer and contains a fixed amount of mass in the inner-layer. Hence we introduce another scaling

$$\xi = \frac{y}{\epsilon(\tau)},$$

and

$$\tilde{U}(\xi, \tau) := \epsilon(\tau)^d U(y, \tau).$$

Then $\tilde{U}(\xi,\tau)$ satisfies

$$\tilde{U}_\tau = \epsilon^{-d(m-1)-2}\big(\Delta \tilde{U}^m - \nabla \cdot (\tilde{U} \nabla (\tilde{U} * \frac{1}{|\xi|^\gamma})\big) + \big(\alpha \nabla \tilde{U} \cdot \xi + \beta \tilde{U}\big) + \dot{\epsilon}\epsilon^{-1}\big(\nabla \tilde{U} \cdot \xi + d\tilde{U}\big). \tag{4.3}$$

After performing this rescaling, we expect $\tilde{U}$ to converge to some stationary blow-up profile $\bar{U}(\xi)$, hence we assume that $\tilde{U}_\tau \to 0$ as $t \to \infty$. As τ goes to infinity, note that the terms on the right hand side of (4.3) are not of the same order, due to the assumption that $\epsilon(\tau)$ slowly decays to 0 as $\tau \to \infty$. Recall that we only consider the case $m \geq 1$, which implies that $\epsilon^{-d(m-1)-2} \gg \dot{\epsilon}\epsilon^{-1} \gg 1$. Hence $\bar{U}$ satisfies the equation

$$\Delta \bar{U}^m - \nabla \cdot (\bar{U} \nabla (\bar{U} * \frac{1}{|\xi|^\gamma})) = 0. \tag{4.4}$$

For Newtonian potential, it is proved in [BCL2] that the only radially symmetric solution to (4.4) has mass M_c, where M_c is the critical mass. That suggests that $\bar{U}$ is the unique stationary solution for (1.1) with critical mass M_c. Hence as $t \to T$, the peak should contain exactly the critical mass M_c, which fits our observation in Figure 10 (b). Moreover, Figure 11 suggests that the rescaled blow-up profile indeed coincides with the stationary solution.

It is an interesting question to solve for the logarithmic corrector $\epsilon(\tau)$; this has been done for $m = 1$ and the Newtonian kernel K in [HV, L, CS], however it is an open problem for general m and K.

5. Numerical Method

The numerical method we use is a combination of a Lagrangian method and an Eulerian method. The main idea is to split the equation (1.1) into two steps, one with the aggregation part only and the next with the diffusion part only, and we run those two steps alternatively. More precisely, in every time step $[t, t+dt]$, we first use the method of characteristic to solve the aggregation equation

$$v_t = -\nabla \cdot (v \nabla (K * v)) \quad \text{for } t \in [t, t+dt], \tag{5.1}$$

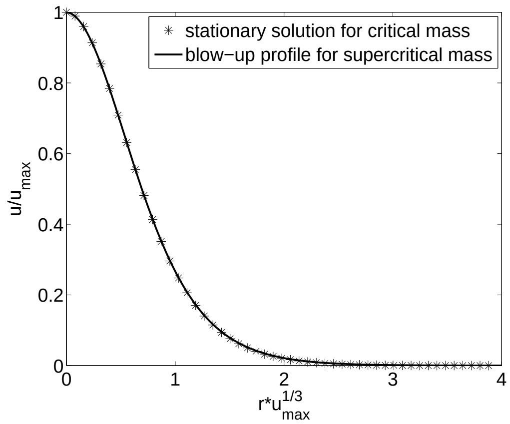

Figure 11: Comparison between the rescaled blow-up profile and the stationary solution with critical mass. The solid line is the rescaled blow-up profile of a a near-self-similar blow-up solution with radially symmetric initial data, with Newtonian potential, $d = 3$ and $m = 4/3$ (critical). The star symbol is the (rescaled) stationary solution with critical mass M_c.

where the time step is chosen to be small enough such that the characteristics do not intersect. After reconstructing the density from the particle locations and performing an adaptive mesh refinement, we then use an implicit finite-difference scheme to solve the following diffusion equation for another time step,

$$w_t = \Delta w^m \quad \text{for } t \in [t, t + dt], \tag{5.2}$$

where the initial data of w is taken from the result of the aggregation step, namely $w(x, t) = v(x, t + dt)$. Then we set $v(x, t + dt) = w(x, t + dt)$ and start the next time step.

5.1. Advection Step

For the advection step, due to the underlying transport structure of (5.1), it can be solved by method of characteristics. To do this we follow the method in [HB1], which we present here for the sake of completeness.

Assume the radial domain is partitioned into the intervals $0 = r_0 < r_1 < \ldots < r_N = R$, where the mass of u is m_i in the ring $B(0, r_{i+1}) \backslash B(0, r_i)$ for $i = 0, \ldots, N - 1$. We then approximate u by a system of N delta rings located at radius $r_0, \ldots, r_N$ with mass $m_1, \ldots, m_N$ respectively. Note that (5.1) is a transport equation, where the outward velocity field at radius r is given by

$$v(r) = -\frac{\partial}{\partial r}(u * K).$$

Hence the ith ring is moving inwards with velocity

$$\frac{d}{dt} r_i(t) = \sum_{j=1}^{N} m_j v_{r_j}(r_i), \tag{5.3}$$

where $v_{r_j}(r_i)$ is the outward velocity at r_i caused by a delta ring with unit mass located at radius r_j. $v_R(r)$ is given by the following integral

$$\begin{aligned} v_R(r) &= -\int_0^\pi K'(\sqrt{R^2+r^2-2rR\cos\theta})\frac{R\cos\theta - r}{\sqrt{R^2+r^2-2rR\cos\theta}}(R\sin\theta)^{d-2}\omega_{d-1}d\theta/(\omega_d R^{d-1}) \\ &= -\gamma\frac{w_{d-1}}{w_d}\int_0^\pi \frac{R\cos\theta - r}{R(R^2+r^2-2rR\cos\theta)^{\gamma/2+1}}(\sin\theta)^{d-2}d\theta, \end{aligned}$$

Due to the homogeneity of the kernel K, we can define $\rho = \dfrac{\min\{r,R\}}{\max\{r,R\}}$, then $v(r)$ becomes

$$v_R(r) = \begin{cases} -\gamma\dfrac{w_{d-1}}{w_d}R^{-\frac{\gamma}{2}-1}I_1(\rho), & \text{if } r \le R \\ -\gamma\dfrac{w_{d-1}}{w_d}r^{-\frac{\gamma}{2}-1}I_2(\rho), & \text{if } r > R, \end{cases}$$

where the two auxiliary functions $I_1(\rho), I_2(\rho)$ are defined by

$$\begin{aligned} I_1(\rho) &= \int_0^\pi \frac{\cos\theta - \rho}{(1+\rho^2-2\rho\cos\theta)}(\sin\theta)^{d-2}d\theta, \\ I_2(\rho) &= \int_0^\pi \frac{\rho\cos\theta - 1}{(\rho^2+1-2\rho\cos\theta)}(\sin\theta)^{d-2}d\theta, \end{aligned}$$

and we only need to perform numerical integration for $I_1(\rho)$ and $I_2(\rho)$ once, for $0 \le \rho \le 1$, which reduce the complexity to $O(N^2)$ to evaluate the right hand side of (5.3). Once we have the velocity of each delta ring in (5.3), we use the classical forth order Runge-Kutta method to evaluate the position at the next time step.

5.2. Regridding and Interpolation

5.2.1. Reconstruct density from particle locations

After the aggregation step, we have new locations of the $\delta-$rings. Assume the i-th $\delta-$ring is now located at radius r_i. We can reconstruct the density u from the particle location as following. We denote by $\bar{u}_i$ the the average density in the ring $[r_i, r_{i+1}]$, then $\bar{u}_i$ is given by $\frac{m_i}{|B(0,r_{i+1})\setminus B(0,r_i)|}$, where m_i is the mass of the i-th δ-ring.

5.2.2. Adaptive mesh refinement

Since we are interested in the blow-up profile, we perform an adaptive mesh refinement that efficiently captures the scaling of the blow-up without losing resolution.

Figure 12 shows that for both self-similar blow-up and non-self-similar blow-up, the density changes slowly outside of the singularity area, due to the fact that the blow-up is localized. Thus we dedicate a fixed portion of the grid to the singularity area and a fixed portion outside of that area.

More precisely, we first find the peak location r_{max}, then we locate the peak area $[r_1, r_2]$ to be the part where $u(r) \ge u(r_{max})/1000$. This interval would contain the singularity area

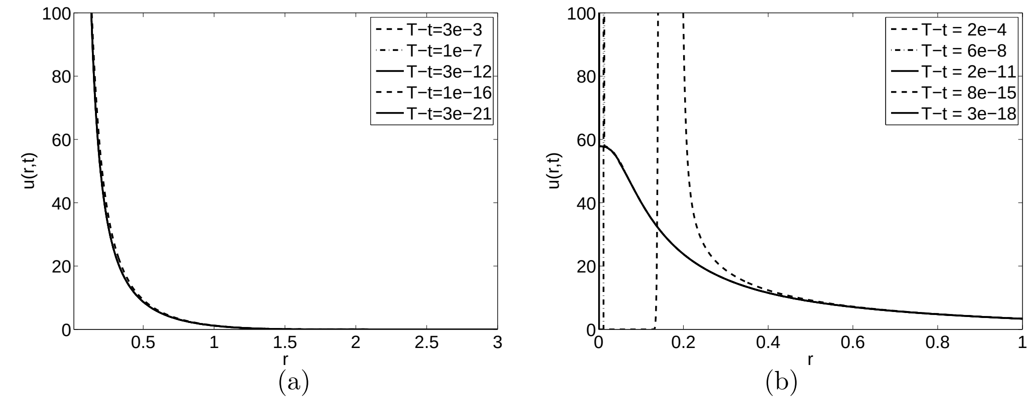

Figure 12: Behavior of solutions away from the blow-up point, where $d = 3, \gamma = 1$ and $m = 1.2$. Figure (a) shows the tail of solution in the case of self-similar blow-up, and Figure (b) is for non-self-similar blow-up.

in the case for the self-similar blow-up, but to make it also work for the non-self-similar blow-up, we enlarge the interval to $[r_L, r_R]$, where $r_L = \max\{0, r_{max} - 2(r_{max} - r_1)\}$, $r_R = r_{max} + 2(r_2 - r_{max})$).

We start with an initial grid of $N = N_0$ points, in the example here $N_0 = 500$. After locating the interval $[r_L, r_R]$ using the method above, we partition $[r_L, r_R]$ into $N/2$ equal-length grids, and partition the remaining set $[0, a] \backslash [r_L, r_R]$ into another $N/2$ equal-length grids. Note that the length of $[r_L, r_R]$ will go to zero as the time approaches the blow-up time, so the grid size inside the interval $[r_L, r_R]$ will be much smaller than outside, which might introduce some numerical error. To ensure that the size of two neighboring grids are comparable, we refine the grid using the strategy similar to [B]: when the size of an outer grid is two times more than the size of its neighboring inner grid, we divide the k inner-most outer grids in half. We perform this procedure iteratively until all neighboring intervals have ratio between 1/2 and 2. We point out that the grid size depends logarithmly on ρ_{max}: In the computation we choose $k = 8$, and the size of the grid grows from 500 to around 900 as the maximum density reaches 10^{50}.

5.2.3. Interpolation

Regridding is followed by interpolation. Given the old cell average $\bar{u}_i$, we will interpolate $u(r)$ for $0 \le r \le a$, then we could use $u(r)$ to compute the cell average u_i' on the new grid.

One way to perform the interpolation is to simply let $u(\frac{r_i + r_{i+1}}{2}) = \bar{u}_i$ and apply a cubic spline interpolation. However, this interpolation does not preserve the mass, nor does it preserve positivity. On the other hand, the simplest mass and positivity preserving interpolation is to make $u(r)$ a piecewise function with value $\bar{u}_i$ in the i-th ring. However this method is only first-order accurate, and we hope to find some more accurate interpolation method that is volume-preserving. More precisely, given the old cell average $\bar{u}_i$, our goal is to find $u(r)$, such that

$$\begin{aligned} \text{minimize} \quad & \int_{B(0,r)} |\nabla u|^2 dx \\ \text{subject to} \quad & u(r) \geq 0 \text{ for } 0 \leq r \leq a \\ \text{and} \quad & \int_{B(r_{i+1})\backslash B(r_i)} u(x)dx = \bar{u}_i |B(r_{i+1})\backslash B(r_i)| \end{aligned} \tag{5.4}$$

We realize that this kind of interpolation is a 1D and simpler version of the pycnophylactic interpolation performed in [T], which we will briefly describe here.

To find the solution to the minimization problem (5.4), we use a finite volume scheme to solve the heat equation $u_t = \Delta u$ on the refined mesh, where the initial data are taken to be the piecewise constant function with value $\bar{u}_i$ on each old grid. After each time step, we adjust u such that both the positivity and the volume-preserving restrictions are met. More precisely, we add a different constant to the value in each old cell, to ensure the density is non-negative and the mass in every old cell remain unchanged. Then we repeat the above steps again until the $u(r)$ does not change.

5.3. Degenerate Diffusion Step

To solve the porous medium equation (5.2) on a fixed grid, we apply a fully implicit finite-volume scheme, and use Newton's method for solving the nonlinear equation. While these are standard procedures for dealing with degenerate diffusion equation (see [KA] for example), we briefly sketch the details here for the sake of completeness.

Assume the radial domain is partitioned into the intervals $0 = r_0 < r_1 < \ldots < r_N = R$. We denote by $U_i(t)$ the average of $u(x,t)$ in the ring $B(0, r_{i+1})\backslash B(0, r_i)$ at time t, and denote by $\vec{U}(t)$ the vector $(U_0(t), \cdots, U_{n-1}(t))$. Our goal is to find $\vec{U}(t + \Delta t)$, such that it solves the following nonlinear equation

$$\frac{\vec{U}(t + \Delta t) - \vec{U}(t)}{\Delta t} = A[\vec{U}^m(t + \Delta t)], \tag{5.5}$$

here A is a finite-volume discretization of the Laplace operator in radial coordinates, and the m-th power in $\vec{U}^m$ is understood in a component-wise sense.

We first explicitly write down the linear operator A. For any radially symmetric function $v(x)$, note that the radial derivative at r_i can be approximated by

$$\partial_r v(r_i) \approx \frac{V_i - V_{i-1}}{(r_{i+1} - r_{i-1})/2} \text{ for } 1 \leq i \leq N-1,$$

where V_i is the average of $v(x)$ in the ring $B(0, r_{i+1})\backslash B(0, r_i)$. For the radial derivative at the boundaries, we have $\partial_r v(x_0) = \partial_r v(x_N) = 0$. Note that divergence theorem gives

$$\int_{B(0,r_{i+1})\backslash B(0,r_i)} \Delta v dx = \partial_r v(r_{i+1})|\partial B(0, r_{i+1})| - \partial_r v(r_i)|\partial B(0, r_i)|.$$

Hence

$$(AV)_i = \frac{\left(\frac{v_{i+1}-v_i}{(r_{i+2}-r_i)/2}\right) r_{i+1}^{d-1} - \left(\frac{v_i - v_{i-1}}{(r_{i+1}-r_{i-1})/2}\right) r_i^{d-1}}{(r_{i+1}^d - r_i^d)/d} \text{ for } 1 \le i \le N-2,$$

and for the two boundaries we have

$$(AV)_0 = \frac{(v_1 - v_0)2d}{r_1 r_2},$$

$$(AV)_{N-1} = -\left(\frac{v_{N-1}-v_{N-2}}{(r_N - r_{N-2})/2}\right) \frac{r_{N-1}^{d-1}}{(r_N^d - r_{N-1}^d)/d}.$$

Next we use Newton's method to solve for $\vec{U}(t+\Delta t)$, where the iteration is performed as follows. For the initial step, we take $\vec{U}^{(0)}$ as $\vec{U}(t)$. Assuming $\vec{U}^{(k)}$ is known, by linearizing $\vec{U}^m(t+\Delta t)$ around $\vec{U}^{(k)}$, we obtain

$$\vec{U}^m(t+\Delta t) \approx m(\vec{U}^{(k)})^{m-1}\vec{U}(t+\Delta t) - (m-1)(\vec{U}^{(k)})^m,$$

hence $\vec{U}^{(k+1)}$ is given by

$$\vec{U}^{(k+1)} = \Big(1 - m\Delta t A(\vec{U}^{(k)})^{m-1}\Big)^{-1}\Big(\vec{U}(t) - (m-1)\Delta t A(\vec{U}^{(k)})^m\Big). \tag{5.6}$$

We point out that it only takes $O(N)$ steps to invert the $N\times N$ matrix $1-m\Delta t A(\vec{U}^{(k)})^{m-1}$, due to its tridiagonal nature. Making use of (5.6), we solve for $\vec{U}^{(k+1)}$ iteratively for $k = 0, 1, \ldots$, until some $\vec{U}^{(k+1)}$ approximately solves (5.5) with error below some predetermined threshold. Then we stop the iteration and simply let $\vec{U}(t+\Delta t) = \vec{U}^{(k+1)}$. Typically the iteration would stop in less than 10 iterations, since the Newton's method has quadratic convergence.

5.4. Adaptive time step

Finally, when the computation in one time step is finished, we update Δt to control the growth rate of the maximum density. In the computation we would multiply Δt by 1.1 if the maximum density increases less than 0.02% in one time step, and divide Δt by 1.1 if the maximum density increases more than 0.1%. We point out that this simple criteria is indeed sufficient for our problem, due to the self-similarity of solutions in the peak area. Figure 13 shows an example of a log-log plot of the time step versus the maximum density.

6. Conclusions and Remarks

We have studied the blowup behavior of radial solutions to the aggregation-diffusion equation $u_t = \Delta u^m - \nabla\cdot(u\nabla K * u)$ in dimension $d \ge 3$ for the kernel $K(x) = |x|^{-\gamma}$, where K is either equal to or less singular than the Newtonian kernel, i.e. $\gamma \le d-2$. Note that the dimension $d = 2$ is omitted in this paper, since when $d = 2$ and K satisfies the above condition,

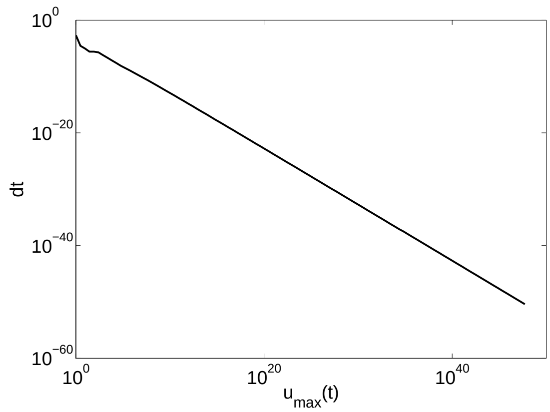

Figure 13: Log-log plot of the time step versus the maximum density, where $d = 3, \gamma = 1$ and $m = 4/3$. In the asymptotic regime, the best fit has slopes of value -1.003, which is in good agreement with the theoretically predicted value -1.

(1.1) is either the well-studied Patlak-Keller-Segel model, or in the subcritical regime where solutions do not blow-up. For $d \geq 3$, formal asymptotic results and numerical observations both show that for supercritical m (i.e. $1 < m < \frac{d+\gamma}{d}$), the solution may blow-up either self-similarly or like a Burger shock; while for critical m (i.e. $m = \frac{d+\gamma}{d}$) and supercritical mass, the solution exhibits a near-self-similar blow-up behavior.

A number of problems regarding the blow-up behavior of solutions remain unsolved. First, for supercritical m, numerical observation suggests that when m, d and γ are fixed, there is a stable self-similar blow-up profile, and at least one unstable self-similar blow-up profile (see Figure 8). It would be interesting to know whether there exists a stable blow-up profile that attracts all self-similar blow-up solutions. For the case $m = 1$ with Newtonian potential, the stability of blow-up profile is studied in [BCKSV]. They proved that there exist a countable family of self-similar blow-up modalities $\{H_n\}$ for $n = 0, 1, 2, ...$, where H_0 gives a stable blow-up profile, and all the other H_n are unstable. However their eigenvalue method does not directly generalize to our equation, due to the nonlinear diffusion term.

For critical m with supercritical mass, numerical observation suggests that the solution may blow-up in a near-self-similar way, however the exact scaling for the blow-up remains open. Although the scaling is derived for $m = 1, d = 2$ and Newtonian potential K in [HV, L, CS], their arguments does not generalize to (1.1) for $m > 1$. Here the difficulty lies in the nonlinear diffusion term, and also in the fact that unlike the $m = 1$ case, the stationary solution with $m > 1$ has a compact support.

The numerical method is an arbitrary Lagrangian Eulerian method with adaptive mesh refinement. The advantage of our method is that we can compute to very high spatial resolution. Using around 1000 spatial points, we can compute the solution until the maximum density reaches 10^{80} and the characteristic spatial scale of the solution reaches 10^{-27}. We point out that our method preserves the L^1 norm of the solution, which is an important property especially for critical m, since the behavior of the solution depends on its mass.

Finally we note that it would be interesting to try to apply the numerical method to other problems that also have a non-local term with power-law interaction. Although the local well-posedness result in [BRB] is only established for kernels K that are less singular than (or equal to) the Newtonian kernel, preliminary numerical results suggests that our algorithm also works when K is more singular than Newtonian kernel. Thus we might be able to apply our numerical method to the fractional porous medium equation introduced in [CV], which is an aggregation equation with a repulsive kernel $K = -|x|^{-\gamma}$, where $2 - d < \gamma < d$.

Acknowledgements

We would like to thank Wangyi Liu for his helpful advice. The authors were supported by NSF Grants EFRI-1024765 and DMS-0907931.

References

[B] A. L. Bertozzi, Symmetric Singularity Formation in Lubrication-Type Equations for Interface Motion, *SIAM J. Applied Math.*, 56(1996):681-714.

[BCL1] A. L. Bertozzi, J. A. Carrillo and T. Laurent, Blow-up in multidimensional aggregation equations with mildly singular interaction kernels, *Nonlinearity*, 22(2009):683-710.

[BCKSV] M. P. Brenner, P. Constantin, L. P. Kadanoff, A. Schenkel and S. Venkataramani, Diffusion, attraction and collapse, *Nonlinearity* 12(1999): 1071-1098.

[BCC] A. Blanchet, V. Calvez and J. A. Carillo, Convergence of the mass-transport steepest descent scheme for the subcritical Patlak-Keller-Segel model. *SIAM J. Numer. Anal.* 46(2008): 691-721.

[BCL2] A. Blanchet, J. A. Carrillo and P. Laurençot, Critical mass for a Patlak-Keller-Segel model with degenerate diffusion in higher dimensions, *Calc. Var.*, 35(2009):133-168.

[BCM] A. Blanchet, J. A. Carrillo and N. Masmoudi, Infinite time aggregation for the critical Patlak-Keller- Segel model in $\mathbb{R}^2$. *Comm. Pure Appl. Math.,* 61(2008):1449-1481.

[BL] A. Blanchet and Ph. Laurençot, Finite mass self-similar blowing-up solutions of a chemotaxis system with non-linear diffusion, To appear in *Comm. Pure Appl. Math.* (2010).

[BCR] C. J. Budd, R. Carretero-González and R.D. Russell, Precise computations of chemotactic collapse using moving mesh methods. *J. Comp. Phys.*, 202(2005): 463-487.

[BK] J. Bedrossian and I. Kim, Global existence and finite time blow-up for critical Patlak-Keller-Segel models with inhomogeneous diffusion. Preprint, *arXiv:1108.5301, 2011.*

[BRB] J. Bedrossian, N. Rodríguez and A.L. Bertozzi, Local and global well-posedness for aggregation equations and Patlak-Keller-Segel models with degenerate diffusion, *Nonlinearity*, 24(2011):1683-1714.

[CV] L. A. Caffarelli and J. L. Vázquez, Nonlinear porous medium flow with fractional potential pressure, preprint, *arXiv:1001.0410*, 2010.

[CS] P.-H. Chavanis and C. Sire, Virial theorem and dynamical evolution of self-gravitating Brownian particles in an unbounded domain. I. Overdamped models, *Phys. Rev. E*, 73(2006), 066103.

[DP] J. Dolbeault and B. Perthame, Optimal critical mass in the two dimensional Keller-Segel model in $\mathbb{R}^2$, *C. R. Acad. Sci. Paris,* 339(2004):611-616.

[E] Y. Epshteyn, Discontinuous Galerkin methods for the chemotaxis and haptotaxis models. *J. Comp. App. Math.*, 224(2009):168-181.

[EI] Y. Epshteyn and A. Izmirlioglu, Fully discrete analysis of a discontinuous finite element method for the Keller-Segel chemotaxis model. *J. Sci. Comp*, 40(2009):211-256.

[EK] Y. Epshteyn and A. Kurganov, New interior penalty discontinuous Galerkin methods for the Keller-Segel chemotaxis model. *SIAM J. Numer. Anal.*, 47(2008):386-408.

[Fa] I. Fatkullin, A study of blow-ups in the Keller-Segel model of chemotaxis. Preprint, *arXiv:1006.4978*, 2011.

[Fi] F. Filbet, A finite volume scheme for the Patlak-Keller-Segel chemotaxis model. *Numerisch. Math.*, 104(2006):457-488.

[GK] Y. Giga and R. Kohn, Nondegeneracy of blowup for semilinear heat equations, *Comm. Pure Appl. Math.*, 42(1989):223-241.

[HB1] Y. Huang and A. L. Bertozzi, Self-similar blowup solutions to an aggregation equation in R^n, *SIAM J. Appl. Math.*, 70(2010):2582-2603.

[HB2] Y. Huang and A. L. Bertozzi, Asymptotics of Blowup Solutions for the Aggregation Equation, to appear in *Discrete Contin. Dyn. Syst.*.

[HS] J. Haskovec and C. Schmeiser, Stochastic particle approximation for measure valued solutions of the 2D Keller-Segel system, *J. Stat. Phys.*, 135(2009):133-151.

[HV] M. A. Herrero and J. L. Velazquez, Chemotactic collapse for the Keller-Segel model, *J. Math. Biol.,* 35(1996):177-194.

[H] D. Horstmann, From 1970 until present: the Keller-Segel model in chemotaxis and its consequences. *I, Jahresber. Deutsch. Math.-Verein.*, 105(2003):103-165.

[KA] P. Knabner and L. Angermann, *Numerical Methods for Partial Differential Equations*, Texts in Applied Mathematics, Vol. 44. Springer-Verlag, Berlin, Heidelberg, New York, 2003.

[KS] N. Kavallaris and P. Souplet, Grow-up rate and refined asymptotics for a two-dimensional Patlak-Keller-Segel model in a disk, *SIAM J. Math. Anal.*, 40(2008/09):1852-1881.

[L] P. M. Lushnikov, Critical chemotactic collapse, *Physics Letters A*, 374(2010):1678-1685.

[M] A. Marrocco, 2D simulation of chemotactic bacteria agreggation, *ESAIM: Math. Model. Numer. Anal.*, 37(2003):617-630.

[S1] Y. Sugiyama, Global existence in sub-critical cases and finite time blow-up in super-critical cases to degenerate Keller-Segel systems, *Diff. Int. Eqns.*, 19(2006):841-876.

[Sa] N. Saito, Conservative upwind finite element method for a simplified Keller-Segel system modelling chemotaxis, *IMA J. Numer. Anal.*, 27(2007):332-365.

[SS] N. Saito and T. Suzuki, Notes on finite difference schemes to a parabolic-elliptic system modelling chemotaxis, *Appl. Math. Comp.*, 171(2005):72-90.

[T] W. R. Tobler, Smooth Pycnophylactic Interpolation for Geographical Regions. *J. Am. Stat. Assoc.*, 74(1979):519-530.